Exploration of third order nonlinear optical features of CuO/PVA-PEG polymer nanocomposites

K. Kannan[a,b,*], S. Agilan[b], P. Peulakumari[c], G. Saveetha[d]
[a]*Department of Physics, M.Kumarasamy College of Engineering, Karur - 639113, Tamilnadu, India*
[b]*Department of Physics, Coimbatore Institute of Technology, Coimbatore – 641014, Tamilnadu, India*
[c]*Department of Physics, Chikkanna Government Arts College, Tiruppur - 641 602, Tamil Nadu, India*
[d]*Department of Mathematics, Kongunadu College of Engineering and Technology, Thottiam, Trichy – 621215, Tamilnadu, India*

CuO/PVA-PEG nanocomposites were prepared by solvent casting method. In XRD spectra, the shifting of peak position and the absence of remaining characteristics peaks of CuO nanoparticles in CuO/PVA-PEG indicates the formation exfoliated nanocomposites. The SEM image reveals the complete dispersion of the nanofillers in polymer matrix. FTIR spectra revealed the formation of strong H-bonds between PVA and PEG during mixing. The absorption and transmission properties of the sample were studied by UV-Vis studies. Z-scan analysis confirms the presence of two-photon absorption in the sample. The synthesized polymer nanocomposite exhibits optical nonlinearity due to the exciton-exciton interaction.

(Received December 20; 2022; Accepted March 13, 2023)

Keywords: Polymer nanocomposites, Nonlinear optics, UV-Vis, Z-scan, Third harmonic generation

1. Introduction

Nonlinear optics deals with the interaction of light with a medium. Most of the linear optical properties of materials are independent of the intensity of incident light. However, if a medium is illuminated by a high intensity light beam and it becomes intensity dependent then the medium is termed as a nonlinear optical medium. Nonlinear optical phenomena have facilitated a wide range of applications, including laser frequency conversion, optical signal processing, ultrafast electro-optical modulation, laser amplifiers and-so-on [1]. Future optical device applications require materials with high third-order optical nonlinearity and rapid response time [2].

The fabrication of polymeric matrices embedded with nanoparticles has recently attracted the attention of researchers working in the field of nonlinear optics [3]. Polymer nanocomposites have attracted a great deal of scientific and technological interest in recent years due to the many advances made possible by the combination of a polymeric matrix and an inorganic nanomaterial in general. Some of the improved features in polymer nanocomposites include tensile properties, wear resistance, elasticity, electrical and thermal conductivity, high heat resistance, and strong barrier to moisture and gases.

Polyvinyl alcohol (PVA) is one of the promising polymer matrix possessing transparency in visible region, excellent elasticity, photo induced response property, water solubility and non-toxic and these make PVA as a potential host material for nanofillers. Further polyethylene glycol (PEG) also has water solubility, low toxicity and shows complex surfactant behavior [4]. PVA and PEG polymer blends have been extensively studied for usage in a variety of applications [5]. When fluid mixtures of PVA and PEG polymers are produced, the hydroxyl groups of PVA

* Corresponding author: kannankgv86@gmail.com
https://doi.org/10.15251/DJNB.2023.181.367

interact with the ether linkage of PEG chains via hydrogen bonding [6]. The porosity of the PVA scaffold can be modified by mixing it with PEG, which is also suitable for increasing the thermosetting foam of pure PVA [7].

Copper oxide (CuO) quantum dots have unique electrical, optical and gas sensing properties. Due to its good electrochemical properties, it can be synthesized using low-cost techniques [8]. Several studies have reported that CuO nanoparticles are the transition metal oxides that show excellent nonlinear optical properties [9-11]. The main objective of this study is to investigate the third-order optical nonlinearity of CuO nanoparticles incorporated PVA-PEG polymer nanocomposites and compare its nonlinear refractive index, nonlinear absorption co-efficient, and third-order nonlinear susceptibility with existing NLO materials.

2. Preparation

2.1. CuO nanoparticles (NPs)

CuO NPs were prepared by sol-gel technique using $CuCl_2$ as precursor. 0.1 M of NaOH was added slowly with 0.1 M of precursor under stirring for 4 hr and the obtained black precipitate was cleaned multiple times by deionized water and ethanol. It was dried at 80–90 ℃ for 14 hr and calcined at 500 ℃ for 4 hr.

2.2. Polymer nanocomposites

The solvent casting method was used to prepare the CuO/PVA-PEG polymer nanocomposite. Initially, 2 g of PVA was dissolved in the distilled water under steady stirring condition maintained at 70℃. The homogeneous solution was then mixed with PEG 600 under the same conditions. Solvent casting was carried out by adding 1% wt of synthesized CuO NPs to the polymer blend kept at 60℃. The mixture was stirred for 1 hr. After 1 hr, the colloid was permitted to cool by pouring onto petri-dish. Five days later, the film of CuO/PVA-PEG polymer nanocomposite was obtained and the film was peeled out for further investigations.

3. Experimental

X-ray diffraction pattern was obtained for CuO/PVA-PEG nanocomposites using PANalytical/Xpert3 diffractometer with Cu$K\alpha$1 irradiation of wavelength 1.54060 Å. The surface morphology and size of the synthesized CuO/PVA-PEG film were recorded using a CAREL ZEISS EVO-18 SEM instrument. FTIR spectrum of the polymer nanocomposite was recorded using PERKIN ELMER Spectrum RX I instrument in the wave number range 4000 cm^{-1} to 400 cm^{-1}. The optical band gap and linear optical properties of CuO/PVA-PEG polymer nanocomposites were studied using Lambda 35, PERKIN ELMER spectrophotometer in the wavelength range from 190 nm to 1100 nm.

The third-order optical linearity of the fabricated sample was analyzed using a Z-scan instrument driven by a semiconductor-continuous wave laser with a wavelength of 532 nm.

4. Results and discussions

4.1. XRD analysis

Fig. 1 shows the XRD peaks of fabricated polymer nanocomposite. The semi-crystalline nature of PVA and crystalline nature of CuO are affected by PEG. The PVA shows diffraction peak at 19.3° [12-13]. The peak at 35.6° confirms the existence of CuO nanoparticles [14]. The shifting of the position of CuO/PVA-PEG peak in XRD pattern and the absence of remaining characteristics peaks of CuO nanoparticles in CuO/PVA-PEG polymer nanocomposite indicates the formation of amorphous nature in sample that results in the production of exfoliated nanocomposite.

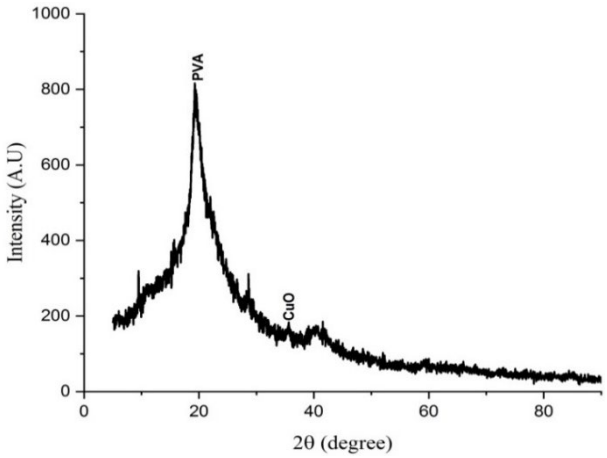

Fig. 1. XRD pattern of CuO/PVA-PEG.

4.2. SEM analysis

The surface morphology of the synthesized CuO/PVA-PEG film is shown in Fig. 2 The SEM image shows that the CuO nanoparticles are tightly attached to the PVA-PEG film, exhibiting a rather smooth surface and the addition of nanofiller to the polymer mixture has definitely changed the morphology of PVA-PEG (Fig. 2).

It is observed that the CuO nanoparticles have a spherical shape completely dispersed throughout the PVA-PEG mixture. A small amount of aggregation of CuO nanoparticles in the polymer blend is observed. The average size of agglomerated CuO nanoparticles is found to be 77 nm. Addition of nanofiller increases the degree of roughness of the film surface [15].

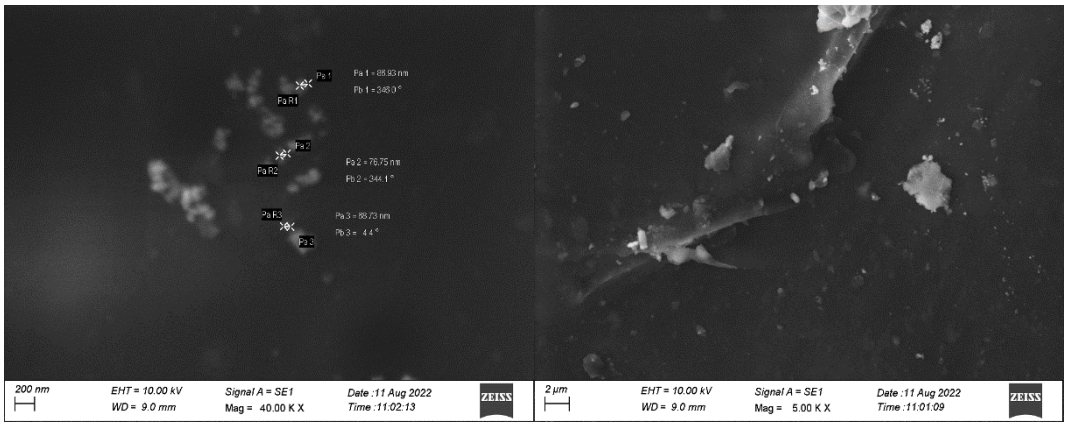

Fig. 2. SEM picture of CuO/PVA-PEG.

4.3. FTIR analysis

FTIR spectrum of the polymer nanocomposites is shown in Fig. 3 Many important bands are observed from the FTIR spectrum at 3482 cm^{-1}, 3101 cm^{-1}, 2951 cm^{-1}, 2168 cm^{-1}, 1733 cm^{-1}, 1647 cm^{-1}, 1575 cm^{-1}, 1462 cm^{-1}, 1141 cm^{-1}, 1319 cm^{-1}, 1038 cm^{-1}, 958 cm^{-1}, 856 cm^{-1}, 719 cm^{-1}, 690 cm^{-1}, 628 cm^{-1} and 575 cm^{-1}. The wide and extreme bands detected around 3000 cm^{-1} to 3500 cm^{-1} has been attributed to – OH group stretching vibrations which result from the formation of strong H-bonds between PVA and PEG during the blending. The small variation in band position and intensity are ascribed to the formation of H-bonding and stretching in water molecules related to CuO (Falqi et al 2018). The band corresponding to the CH_2 symmetric stretching mode is identified at 2951 cm^{-1} [16]. The strong C=O stretching is noticed at the band position 1733 cm^{-1} and 1647 cm^{-1} [17]. The characteristic band at 1575 cm^{-1} is assigned to the C=C stretching

vibration [18]. The absorption bands at 1420 and 1319 cm^{-1} are attributed to CH_2 bending and CH_2 wagging vibrations of PVA [19]. C-H bending vibration gives rise to the band at 1141 cm^{-1}.

The characteristics band corresponding to the stretching vibrations of metal oxide in polymer nanocomposites are recorded at 499 cm^{-1}, 523 cm^{-1}, 575 cm^{-1}, 628 cm^{-1} and 690 cm^{-1} which confirms the existence of CuO nanoparticles in the fabricated sample [20-22]. The band recorded at 799 cm^{-1} is ascribed to the C-O stretching vibrations.

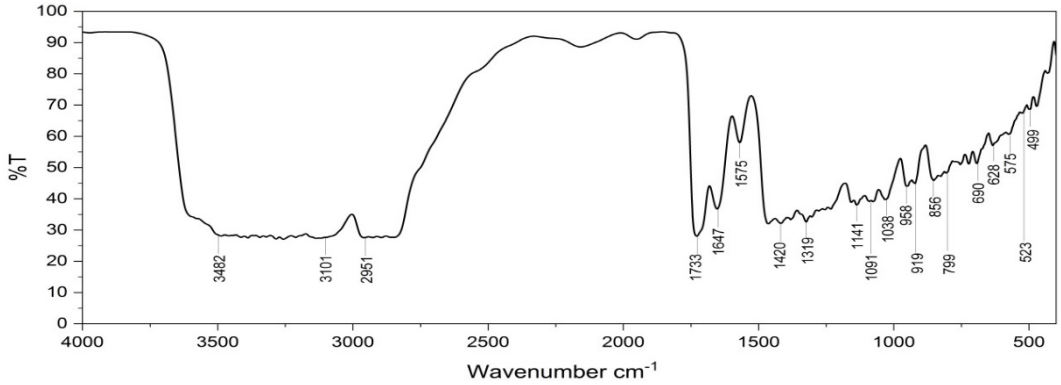

Fig. 3. FTIR spectrum of CuO/PVA-PEG.

Table 1. Assignments of vibrational frequencies of CuO/PVA-PEG.

Observed vibrational bands (cm^{-1})	Assignments
3482	O-H stretching
3101	O-H stretching
2951	CH2 symmetric stretching
1733	C=O stretching
1647	C=O stretching
1575	C=C stretching
1420	CH2 bending
1319	CH2 wagging
1141	C-H bending
1091	C=O stretching
1038	C-C deformation
958	C-C stretching
919	CH2 rocking
856	C-C stretching
799	C-O stretching
500 – 690	Cu-O stretching

4.4 Optical studies

Absorption and transmission spectra of CuO/PVA-PEG are shown Fig. 4(a) and 4(b). Due to the presence of CuO nanoparticles, the prepared nanocomposite shows high absorption of incident photons [23]. It is noted that the prepared polymer nanocomposites have poor

transmittance in both the UV and visible region, indicating moderate transparency by the nanocomposite.

Using band theory, band gap value is obtained. The band gap of the fabricated sample can be measured using the Tauc's relation given as follows.

$$(\alpha h\upsilon)^2 = A(h\upsilon - E_g) \quad (1)$$

The plot was drawn between hυ (eV) and $(\alpha h\upsilon)^2$ for the purpose to find band gap value is shown Fig. 5. The band gap value was found to be 5.2 eV by extrapolating the straight line of the spectra to the x-axis that is $(\alpha h\upsilon)^2 = 0$. This value is slightly lower than the reported energy gap value (5.3 eV) of pure PVA-PEG [16]. This is ascribed to the formation of sub-levels in the forbidden energy gap because of the existence of CuO nanoparticles.

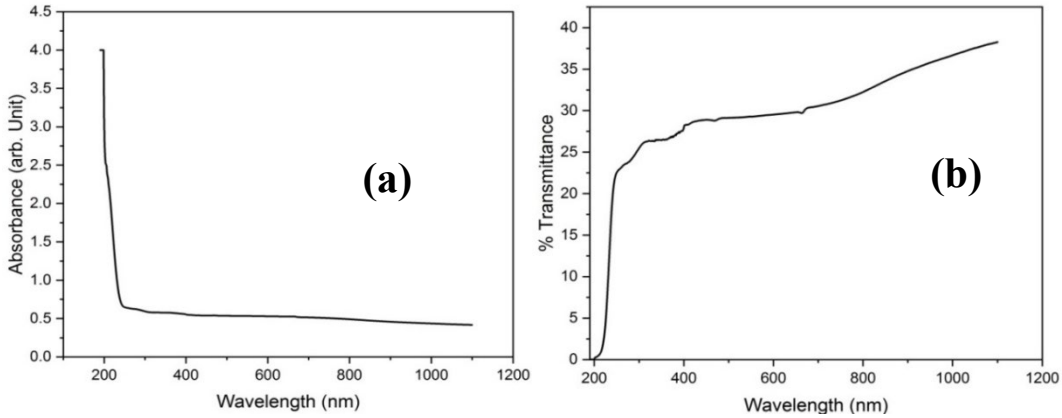

Fig. 4. (a). Optical absorption and (b) transmission spectrum of CuO/PVA-PEG.

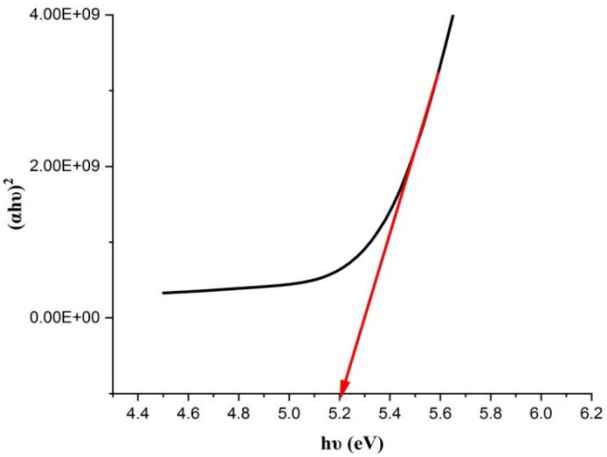

Fig. 5. Plot between hυ vs. $(\alpha h\upsilon)^2$ of CuO/PVA-PEG

The transition in this situation is carried out in two steps and involves the transfer of an electron from the valence band to localized levels and then to the conduction band.

4.5. Third harmonic generation

For measuring the magnitude and sign of nonlinear index of refraction and absorption coefficients of third order optical nonlinearity, Z-scan is a convenient single-beam technique that provides high sensitivity [24]. This approach involves translating the sample through a focused laser beam (Z direction) and measuring the transmittance of the sample with and without aperture (a closed-aperture Z-scan and open aperture Z-scan). The closed-aperture and open-aperture Z-

scan techniques are used to measure the nonlinear index of refraction and the absorption coefficient (β) that are related to the real and imaginary part of the third-order nonlinear optical susceptibility. Fig. 6(a) and Fig. 6(b) depict the closed and open aperture traces of CuO/PVA-PEG polymer nanocomposites respectively.

The relation representing intensity dependent index of refraction is written as

$$n(I) = n_0 + n_2(I) \tag{2}$$

where, n_0 and n_2 are the linear and nonlinear refractive index respectively.

The two photon absorption has been calculated from the formula.

$$\beta = \frac{2\sqrt{2}\Delta T}{I_0 L_{eff}} \tag{3}$$

where, ΔT is the normalized transmittance of the sample at z-position. I_0 is the intensity of incident beam at Z=0. The on-axis phase shift ($|\Delta\phi_0|$) dependence of ΔT is given as

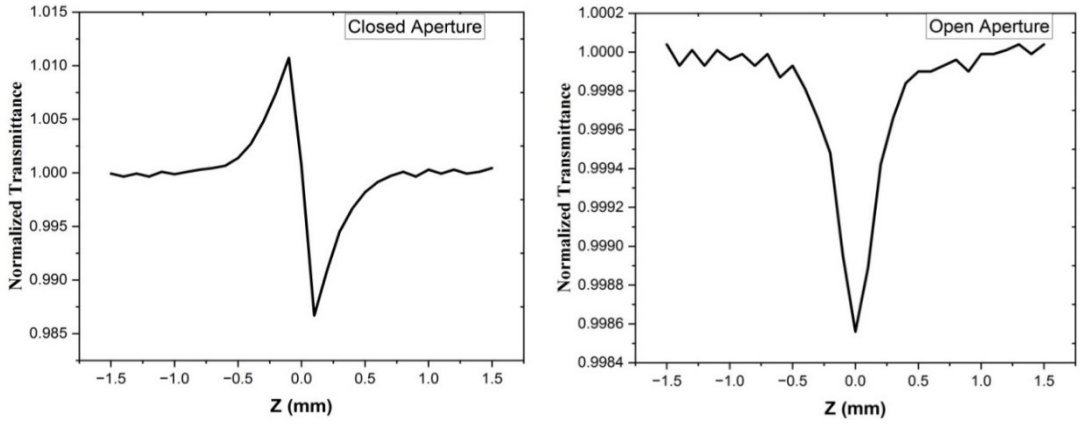

Fig. 6. Z-scan plot of CuO/PVA-PEG in (a) closed aperture and (b) open aperture.

$\Delta T_{p\text{-}v} = 0.406(1\text{-}S)^{0.25} |\Delta\phi_0|$ where, $S = 1 - e^{(-2r_a^2 / \omega_a^2)}$ in which r_a and ω_a indicates aperture and beam radius respectively. By knowing the value of $|\Delta\phi_0|$, n_2 is calculated using the relation,

$$n_2 = \frac{\Delta\phi_0}{K I_0 L_{eff}} \tag{4}$$

In this relation, $L_{eff} = (1 - e^{-\alpha L})/\alpha$ is the effective thickness of the nanocomposite. The wave number is written as $K = 2\pi / \lambda$, where λ is the wavelength the incident laser beam.

The linear refractive index is calculated using the relation:

$$\alpha = \frac{2.303 log\left(\frac{1}{T}\right)}{t} \tag{5}$$

The observed transmittance shows a decline in the traces of the open aperture Z-scan, indicating reverse saturation absorption. Similarly, in closed aperture Z-scan, there is a peak at the beginning followed by valley in the transmittance representing negative index of refractive with self-defocusing effect [25].

The real and imaginary part of the third order NLO susceptibility and effective third order NLO susceptibility can be obtained using the following relations. The synthesized polymer nanocomposite exhibits optical nonlinearity due to the exciton-exciton interaction

$$Re\chi^{(3)}\ (esu) = \frac{10^{-4}\varepsilon_0 c^2 n_0^2 n_2}{\pi} \quad (6)$$

$$Im\chi^{(3)}(esu) = \frac{10^{-2}\varepsilon_0 c^2 n_0^2 \lambda\beta}{4\pi^2} \quad (7)$$

$$\left|\chi^{(3)}\right| = \sqrt{Re(\chi^{(3)})^2 + Im(\chi^{(3)})^2} \quad (8)$$

NLO factors such as n_2, β and $\chi^{(3)}$ are essential in determining the reliability of the prepared sample for nonlinear optical applications such as optical switching devices, optical limiters, frequency-shifted lasing, and so on. Nonlinear parameters are comparable to previously reported values. Dong et al 2022 evaluated the nonlinear parameters β, n_2 & $\chi^{(3)}$ of CuO nanosheets for ultrafast generation and they were found to be -0.88 cm/MW, 2.44×10^{-4} cm^2/GW and 1.4×10^{-9} esu repectively. Similarly nonlinear optical values of CuO thin films were found to be n_2 = -3.96×10^{-17} m^2/W, β=-1.69×10^{-10} m/W [10]. The NLO parameters of PS/ZnO/CuO such as β, n_2 & $\chi^{(3)}$ were estimated as 3.118×10^{-7}cm/W, -4.39×10^{-12} cm^2/W & 1.16×10^{-6} esu [26]. This confirmed from previously reported values that CuO/PVA-PEG represents a potential material for optical applications.

Table 2. Z-Scan calculated values of CuO/PVA-PEG.

Parameters	Values
Laser beam wavelength	532 nm
Focal length of the lens	103 mm
Beam radius of the aperture	3.5 mm
Aperture radius	1.25 mm
Sample thickness	0.155 mm
Effective thickness (L_{eff})	0.154 mm
Linear absorption co-efficient (α)	79.43
Nonlinear refractive index (n_2)	6.37×10^{-9} cm^2/W
Nonlinear absorption coefficient (β)	3.70×10^{-4} cm/W
Real part of third order susceptibility Re ($\chi^{(3)}$)	7.34×10^{-6} esu
Imaginary part of third order susceptibility Im ($\chi^{(3)}$)	1.22×10^{-6} esu
Third order optical nonlinear susceptibility ($\chi^{(3)}$)	**$7.44\ 10^{-6}$ esu**

5. Conclusion

Nanofillers were prepared by sol-gel method using appropriate combination of precursors. Incorporation of individual CuO nanofillers into the PVA-PEG polymer blend was carried out by solvent casting method in the colloidal state kept at 70 °C. In the XRD report of the nanocomposites, only a few peaks corresponding to the nanofillers were identified due to the exfoliation of the nanoparticles in the layered structure. Morphological studies were carried out by SEM analysis. It revealed a complete distribution of nanofillers in the polymeric matrix and they have a very smooth surface. FTIR spectrum was used to detect various functional groups in polymer nanocomposites. The third order nonlinear optical susceptibility of the title compound is 7.44 × 10-6 esu, which shows CuO/PVA-PEG as a potential material for optical applications.

References

[1] Y. Zhao, Y. Yang, H. B. Sun, PhotoniX 2(1), 1 (2021); https://doi.org/10.1186/s43074-021-00025-1

[2] B. Liu, H. Li, C. C. Har, W. Que, Y. L. Loy, C. K. Hin, L. G. Ming, G. X. Qin, Materials Letters 51(6), 461 (2001); https://doi.org/10.1016/S0167-577X(01)00336-6

[3] H. Du, G. Q. Xu, W. S. Chin, L. Huang, W. Ji, Chemistry of Materials 14(10), 4473 (2002); https://doi.org/10.1021/cm010622z

[4] G. Cojocariu, A. Natansohn, Journal of Physical Chemistry B 107(23), 5658 (2003). https://doi.org/10.1021/jp0278465

[5] A. M. El-naggar, Z. Heiba, M. Mohamed, A. M. Kamal, G. Lakshminarayana, A. S. Muhammad, Optik 258, 1 (2022); https://doi.org/10.1016/j.ijleo.2022.168941

[6] C. Sawatari, T. Kondo, Macromolecules 32(6), 1949 (1999); https://doi.org/10.1021/ma980900o

[7] P. Liu, W. Chen, C. Liu, M. Tian, P. Liu, Scientific Reports 9(1), 1 (2019); https://doi.org/10.1038/s41598-019-46061-7

[8] A. Manjunath, M. Irfan, K. P. Anushree, K. M. Vinutha, N. Yamunarani, Advances in Materials Physics and Chemistry 06(10), 263 (2016); https://doi.org/10.4236/ampc.2016.610026

[9] G. S. Boltaev, R. A. Ganeev, P. S. Krishnendu, K. Zhang, C. Guo, Scientific Reports 9(1), 1 (2019); https://doi.org/10.1038/s41598-019-47941-8

[10] A. Chen, G. Yang, H. Long, F. Li, Y. Li, P. Lu, Thin Solid Films 517(15), 4277 (2009); https://doi.org/10.1016/j.tsf.2008.11.139

[11] L. Dong, H. Chu, Y. Li, S. Zhao, D. Li, Journal of Materiomics 8(2), 511 (2022); https://doi.org/10.1016/j.jmat.2021.06.007

[12] H. E. Assender, A. H. Windle, Polymer, 39(18), 4295 (1998); https://doi.org/10.1016/S0032-3861(97)10296-8

[13] H. E. Assender, A. H. Windle, Polymer 39(18) 4303 (1998); https://doi.org/10.1016/S0032-3861(97)10297-X

[14] K. Subashini, S. Prakash, V. Sujatha, Materials Research Express 7(11), 1 (2020); https://doi.org/10.1088/2053-1591/abc979

[15] K. K. Dey, P. Kumar, R. R. Yadav, A. Dhar, A. K. Srivastava, RSC Advances 4(20), 10123 (2014); https://doi.org/10.1039/c3ra46898d

[16] A. A. Alhazime, Journal of Inorganic and Organometallic Polymers and Materials 30(11), 4459 (2020); https://doi.org/10.1007/s10904-020-01577-8

[17] E. M. Abdelrazek, I. S. Elashmawi, A. El-khodary, A. Yassin, Current Applied Physics 10(2), 607 (2010); https://doi.org/10.1016/j.cap.2009.08.005

[18] S. Sagadevan, J. A. Lett, G. K. Weldegebrieal, S. Garg, W. Oh, Catalysts 11(8), 1 (2021); https://doi.org/10.3390/catal11081008

[19] R. M. Ahmed, A. A. Ibrahim, E. A. El-Said, Acta Physica Polonica A 137(3), 317 (2020); https://doi.org/10.12693/APhysPolA.137.317

[20] S. R. Praffulla, S. G. Bubbly, AIP Conference Proceedings 1953, 030168-1 (2018); https://doi.org/10.1063/1.5032503

[21] P. S. Umoren, D. Kavaz, A. Nzila, S. S. Sankaran, S. A. Umoren, Polymers 14(9), 1 (2022); https://doi.org/10.3390/polym14091832

[22] N. R. Dhineshbabu, V. Rajendran, N. Nithyavathy, R. Vetumperumal, Applied Nanoscience, 6, 933 (2016); https://doi.org/10.1007/s13204-015-0499-2

[23] B. H. Rabee, F. Z. Razooqi, M. H. Shinen, Chemistry and Materials Research 7(4), 103 (2015).

[24] M. Sheik-Bahae, A. A. Said, T. H. Wei, T. J. Hagan, E. W. Van-stryland, EEE Journal of Quantum Electronics, 26(4), 760 (1990); https://doi.org/10.1109/3.53394

[25] Y. S. Tamgadge, A. L. Sunatkari, S. S. Talwatkar, V. G. Pahurkar, G. G. Muley, Optical

Materials 51, 175 (2016); https://doi.org/10.1016/j.optmat.2015.11.037
[26] H. M. Shanshool, M. Yahaya, W. M. M. Yunus, I. Y. Abdulla, Opt Quant Electron 49(1), 1 (2017); https://doi.org/10.1007/s11082-016-0830-5